EXPERIMENTAL STUDY AND OPTIMIZATION OF A DISCRETE-ELEMENT–BASED MACADAMIA GREEN-HUSK EXTRUSION-PEELING MACHINE
/
基于离散元的澳洲坚果青皮挤压脱壳机实验研究与优化

Xuyan SONG, Daigen ZHU*), Heng CHENG, Chaobao LIN
College of Mechanical and Transportation Engineering, Southwest Forestry University, Yunnan/China
Corresponding author: Daigen Zhu, Yunnan 650224, China
Tel.: +86-159-8713 4202; Fax: +86-159-8713 4202; Email: zhudg@swfu.edu.cn
DOI: https://doi.org/10.35633/inmateh-78-40

Keywords: *macadamia nut; extrusion peeling; EDEM simulation; response surface optimization; nut integrity; dehusking machine*

ABSTRACT
This study established an integrated experimental–simulation framework for optimizing the green-husk dehusking process of macadamia nuts. The objective was to quantify the effects of drum speed, minimum gap, and feed rate on dehusking performance and nut integrity. The nut damage rate was determined by visual inspection, identifying visible cracks or fractures on the nut surface due to the brittleness of the green husk and the hardness of the nut. Mechanical characterization was conducted through static loading tests in three orthogonal orientations to determine the anisotropic fracture behavior of green husks. Discrete element simulations (EDEM) were calibrated using measured friction, restitution, and density parameters and validated through a repose-angle test. A Box–Behnken design with response surface methodology was applied to evaluate interactive effects among process parameters and derive an optimal operating region. The equivalent peeling force of green husks ranged from 0.30 to 2.00 kN. Drum speed was the dominant factor influencing dehusking efficiency ($p < 0.01$), while minimum gap and feed rate had weaker main effects. The validated model predicted a stable high-performance window at 300–400 r min^{-1}, 9–10 mm minimum gap, and 6–10 kg min^{-1} feed rate. Under optimal conditions (400 r min^{-1}, 9.5 mm, 6.3 kg min^{-1}), the measured dehusking rate reached 95.4% with a nut damage rate of 4.76%. These results demonstrate that the combined experimental–DEM (Discrete Element Method) approach provides a reliable basis for parameter tuning and structural design of macadamia dehusking equipment, enabling improved efficiency and reduced nut damage.

摘要
本研究构建了一种用于优化夏威夷果青壳脱壳过程的试验–仿真一体化框架，旨在定量分析滚筒转速、最小间隙和给料量对脱壳性能及坚果仁完整性的影响。通过在三个正交方向上的静载试验对青壳进行力学表征，以确定其各向异性断裂行为。基于离散元软件 EDEM 的仿真,采用实测的摩擦系数、恢复系数和密度参数进行标定，并通过休止角试验完成验证。利用 Box–Behnken 试验设计结合响应面方法，评估工艺参数之间的交互作用并确定最优运行区间。结果表明，青壳等效剥离力范围 0.30～2.00 kN。滚筒转速是影响脱壳效率的主导因素（$p < 0.01$），而最小间隙和给料量的主效应相对较弱。经验证模型预测，在转速 300～400 r min^{-1}、最小间隙 9～10 mm、给料量 6～10 kg·min^{-1} 条件下存在稳定的高性能工作窗口。在最优工况（400 r min^{-1}、9.5 mm、6.3 kg·min^{-1}）下，实测脱壳率达到 95.4%，仁破损率为 4.76%。
研究结果表明，试验与 DEM（Discrete Element Method，离散元方法）相结合的研究方法，可为夏威夷果脱壳设备的参数整定与结构设计提供可靠依据，从而提高脱壳效率并降低仁破损率。

INTRODUCTION

Macadamia nuts (*Macadamia integrifolia*), known for their distinctive flavor and high nutritional value, hold a prominent position in the international market and serve as one of the major export-oriented specialty forest products in regions such as Yunnan, China. Green husk removal is the primary step in macadamia nut processing *(Yang et al., 2024)*.

Song Xuyan, Master's student in Mechanical Engineering; Zhu Daigen, Professor;
Chen Heng, Master's student in Mechanical Engineering; Lin Chaobao, Master's student in Mechanical Engineering

The efficiency of husk detachment and the nut breakage rate directly affect nut yield, product grading quality, and energy consumption, thereby exerting a decisive influence on industrial production stability and overall economic benefit *(Ma et al., 2025)*.

Systematic reviews of nut postharvest processing emphasize the importance of optimizing equipment parameters to improve peeling efficiency and nut integrity. The macadamia peeling process is highly sensitive to physical properties such as moisture content and nut size, requiring robust equipment design. Researchers have conducted various mechanical tests, such as static loading and shear tests, to model the mechanical response and failure criteria of nut shells and husks, providing a basis for simulation and design *(Han et al., 2024*). Equipment designs like drum-type, roller-type, and guided extrusion-type peeling devices have been widely used, and the effects of drum parameters on peeling rate and nut damage have been explored. However, most studies rely on empirical methods and lack systematic multi-parameter analysis *(Jiang et al., 2021; Shi et al., 2020; Wang et al., 2022*).

In recent years, the Discrete Element Method (DEM) has been applied to nut processing, revealing particle–component interactions and frictional mechanisms. Research by *Cai Zongshou et al.* (*2025*) and *Li Han et al. (2025)* showed DEM's effectiveness in predicting particle forces in peeling mechanisms, but most studies focus on model validation without coupling optimization with experimental data.

International research on macadamia green husk removal and drum-type extrusion peeling is limited, and existing studies focus on mechanical characterization and equipment optimization. These studies identify a trade-off between peeling parameters and nut breakage rate (*Walton and Wallace, 2015*). Despite focusing on structural optimization, previous studies lack comprehensive quantitative analysis of the effects of drum speed, gap, and feed rate. Furthermore, DEM simulations and statistical optimization methods have not been integrated effectively.

This study aims to address these gaps by using a framework that integrates mechanical characterization, EDEM modeling, and response surface optimization (RSM). This approach allows for the visualization and optimization of multi-parameter effects in the peeling process, offering a more efficient and precise solution for improving both peeling efficiency and nut integrity. It overcomes the limitations of traditional empirical testing, providing a theoretical and methodological foundation for nut peeling machinery design.

MATERIALS AND METHODS

Peeling Structure and Principle

Horizontal Single-Drum Guided Extrusion Structure

A horizontal single-drum guided extrusion system was used for macadamia green husk removal (Fig. 1). The machine consists of a top cover, a guiding–peeling drum, an adjustable support plate, a cage mesh, and a frame. Three helical guiding ribs, spaced at 120° intervals on the drum's surface, create a stable rolling and extrusion channel. Between these ribs, three rows of peeling columns, 13 mm in diameter, are aligned, with each row containing nine columns spaced 70 mm apart along the drum axis.

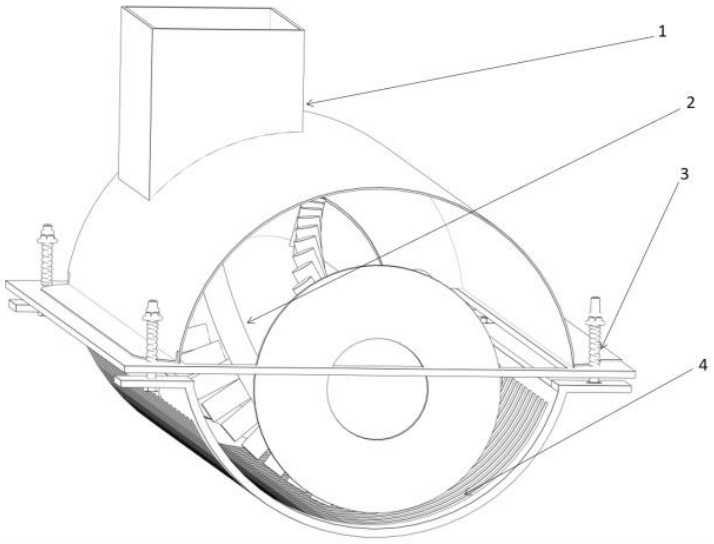

Fig. 1 - Horizontal single–drum guided extrusion structure

1 – Top cover; 2 – Guiding–peeling integrated drum; 3 – Adjustable adaptive support plate; 4 – Cage mesh

The cage mesh is connected to the frame via adjustable bolts, allowing the gap between the drum and the cage to vary from 4 to 12 mm to accommodate different materials. The material is fed from the top, and as the drum rotates, nuts are captured by the guiding ribs and conveyed forward through the helical channel. The nuts enter a narrow extrusion zone where husk cracking and detachment occur under dual-side compression and tangential shear. Husk debris is expelled via centrifugal and gravitational forces, aided by the periodic release of the guiding ribs, preventing secondary clamping or excessive abrasion. The peeled nuts continue moving axially toward the outlet, ensuring continuous operation. The transmission and support frame at both ends of the equipment provide uniform torque and low vibration, maintaining stable rolling and extrusion conditions.

The machine follows a "feeding–guiding–extrusion–screening/discharge" sequence. Nuts roll and slide under guiding ribs, entering a narrow gap where the husk is peeled by compression and shear forces. Husk fragments pass through the mesh, and intact nuts are discharged, ensuring efficient operation *(Hlavangwani et al., 2025*).

Peeling Principle

The macadamia green husk removal process relies on normal compression and tangential friction-shear forces between the drum and support plate. Three helical guiding ribs on the drum surface generate a thrust force, moving the nuts into a narrow extrusion gap. The husk is cracked and peeled under compression and shear forces, with periodic contact between the ribs and peeling columns aiding crack extension. The material moves forward due to the guiding ribs, and the combination of drum rotation and the support plate creates a "rolling-extruding-peeling" cycle. Once the husk is detached, debris is expelled via centrifugal force and the ribs' discharging action. The intact nuts move smoothly to the outlet, completing a continuous peeling process.

In summary, the peeling mechanism involves directional material transport by guiding ribs, a stable compression field from the narrow gap, and the combined effects of normal compression and shear forces.

Mechanical Properties of Macadamia Green Husk

Experimental Preparation

As illustrated in Fig. 2, the hilum line is a distinct morphological feature of the macadamia nut, typically appearing as a shallow groove extending from the nut apex to the stem end. Once the husk is removed, the hard-shelled nut can be approximately regarded as a sphere.

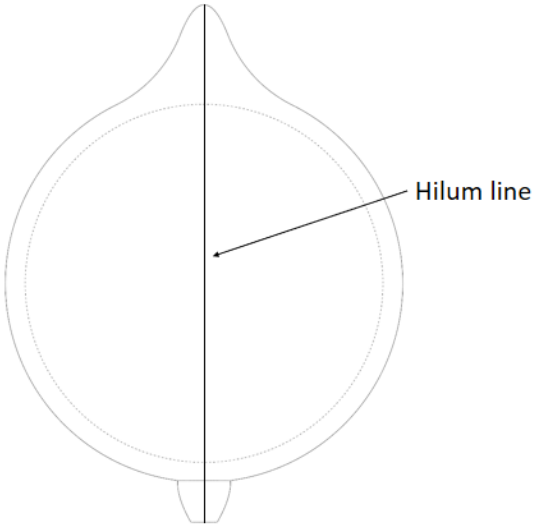

Fig. 2 - Schematic Diagram of the Green Husk of Macadamia Nuts

Based on these characteristics, three orthogonal loading directions were defined for mechanical testing:

When the hilum line is positioned at the top or bottom, the direction is referred to as the hilum direction;

The plane perpendicular to this direction is defined as the normal direction;

The direction perpendicular to both of the above is the lateral direction.

After size screening, the green-husked macadamia nuts were classified into six grades according to their average diameters, as listed below.

Table 1

Macadamia Nut Grades

Grade Code	Average Diameter (mm)
D_1	＞31
D_2	29.5-31
D_3	28-29.5
D_4	26.5-28
D_5	25-26.5
D_6	＜26.5

Note. The macadamia nuts were divided into six size grades according to mean diameter and shell dimensions. Each grade contained more than 30 nuts, which were used in subsequent compression and dehusking tests. Values represent mean ± SD.

The six nut size grades (D_1–D_6) covered the major dimensional range of macadamia nuts harvested during the collection period. According to regional harvesting statistics, nuts in the medium and larger size ranges (D_1–D_3) were selected to ensure experimental relevance and efficiency.

Three loading directions were adopted in the tests: F_1(hilum direction), F_2 (normal direction), and F_3 (lateral direction).

A Bves3100 universal testing machine (Hebei Zhongbo Ruike Instrument Manufacturing Co., Ltd., Hebei, China; rated capacity 100 kN) was used for the mechanical tests. The crosshead displacement rates—1, 7, and 13 mm min^{-1}—were selected for testing.

Fracture Characteristic Analysis

Static mechanical tests were performed using a universal material testing machine in three directions, and the representative force–displacement curves for each direction are shown in Fig. 3.

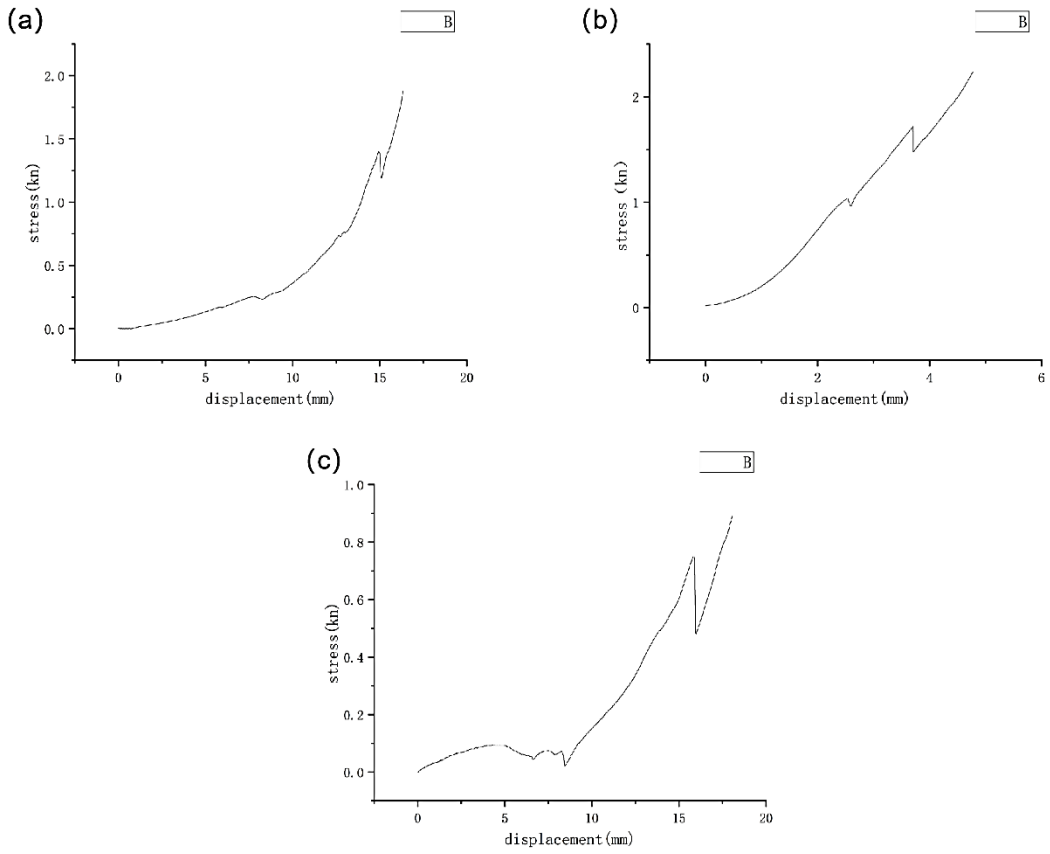

Fig. 3 - Variation with displacement under loads in different directions

The three loading directions showed clear anisotropy:

Hilum direction (a): Medium stiffness and peak load, with axial compression, bending, and shear effects.

Normal direction (b): Highest stiffness and peak load, dominated by axial compression and leading to brittle fracture.

Lateral direction (c): Lowest stiffness and largest displacement, mainly due to bending and shear, with a gradual failure process.

Despite different stress patterns, the fracture mechanism was similar: crack initiation from stress concentration, followed by local buckling or brittle fracture. This highlights the importance of considering direction-dependent stiffness and peak load in stress analysis and fracture modeling (*Ali et al., 2023*).

Extrusion Experiment and Results

Extrusion experiments were conducted with nut size grade (D), loading rate (V), and loading direction (F) as influencing factors. Each factor was set at three levels, and all experiments were repeated three times.

Table 2

Levels of Factors in Extrusion Experiments

Experiment No.	Nut Size Grade	Loading Rate (mm min⁻¹)	Direction of Applied Load
1	D_1	1	F_1
2	D_1	7	F_2
3	D_1	13	F_3
4	D_2	1	F_2
5	D_2	7	F_3
6	D_2	13	F_1
7	D_3	1	F_3
8	D_3	7	F_1
9	D_3	13	F_2

Note. The nut size grades (D_1, D_2, D_3) represent different categories of macadamia nuts based on their average diameter. The loading rate (V) was varied at three levels: 1 mm min⁻¹, 7 mm min⁻¹, and 13 mm min⁻¹. The direction of the applied load (F_1, F_2, F_3) corresponds to different orientations in which the load was applied during the extrusion experiments.

Table 3

Extrusion Test Results

Replicate No.	Nut Size Grade *(Ali et al.)*	Loading Rate (mm min⁻¹)	Direction of Applied Load	Peeling Point Force (N)
1	31.5	1	F_1	1653
2	31.5	1	F_1	1675
3	31.5	1	F_1	1734
1	31.5	7	F_2	1434
2	31.5	7	F_2	1521
3	31.5	7	F_2	1366
1	31.5	13	F_3	339
2	31.5	13	F_3	441
3	31.5	13	F_3	394
1	30	1	F_2	1506
2	30	1	F_2	1466
3	30	1	F_2	1554
1	30	7	F_3	383
2	30	7	F_3	354
3	30	7	F_3	397
1	30	13	F_1	1154
2	30	13	F_1	1425
3	30	13	F_1	1220
1	28.5	1	F_3	291
2	28.5	1	F_3	210
3	28.5	1	F_3	240
1	28.5	7	F_1	997

Replicate No.	Nut Size Grade (*Ali et al.*)	Loading Rate (mm min^{-1})	Direction of Applied Load	Peeling Point Force (N)
2	28.5	7	F_1	1172
3	28.5	7	F_1	906
1	28.5	13	F_2	2214
2	28.5	13	F_2	1871
3	28.5	13	F_2	2210

Note. F represents the equivalent peeling force before the first pronounced drop in the load–displacement curve. Results are given as mean ± SD (n = 3). F1, F2, and F3 correspond to the suture, loading, and lateral directions of loading, respectively.

The equivalent peeling force was defined as the load at the "first significant drop" in the force–displacement curve. Peak loads were approximately 2.3 kN in the normal direction, 1.9 kN along the hilum direction, and 0.9 kN laterally.

Excluding extreme outliers, the robust design range for equivalent peeling force was determined to be 0.30–2.00 kN (300–2000 N). The lower limit ensures reliable crack initiation and continuous peeling, while the upper limit accounts for safety in challenging conditions such as high moisture, unfavorable orientation, or multi-nut feeding (*Zhao and Wang, 2025*).

EDEM Simulation of Macadamia Green Husk Peeling

EDEM Discrete Element Analysis

To further elucidate the force mechanisms and motion behavior of macadamia nuts during the guided extrusion peeling process, EDEM software was employed for discrete element analysis *(Hadi et al., 2024)*.

Determination of Simulation Parameters

To ensure the reliability of EDEM discrete element simulation results, the simulation input parameters must accurately reflect the actual physical properties of the materials. In this study, key parameters such as friction coefficients, restitution coefficients, density, and Poisson's ratio were experimentally measured for both the macadamia husk and its contact interactions with structural components.

Static and Rolling Friction Coefficients

The inclined-plane sliding and rolling methods were used to obtain static and dynamic friction coefficients for husk–husk and husk–45# steel contacts.

The static friction coefficient was obtained by gradually increasing the tilt angle until incipient motion and recording the critical angle:

$$\mu_s = \tan \theta_s \quad (1)$$

Fig. 4 - Experimental Equipment for Inclined Plane Rolling Method 1

The dynamic friction coefficient was calculated by:

$$\mu_k = L_1 \sin\theta / (L_1 \cdot \cos\theta + L_2) \quad (2)$$

Fig. 5 - Experimental Equipment for Inclined Plane Rolling Method 2

Restitution Coefficient

The restitution coefficient E for "husk–husk" and "husk–45# steel" contacts was determined using the free-fall method. The restitution coefficient was calculated as:

$$E = \sqrt{\frac{h_2}{h_1}} \quad (3)$$

Density and Poisson's Ratio

The density was calculated as:

$$\rho_s = m_s/Vs \quad (4)$$

For the determination of Poisson's ratio, husk strips (gauge length L_0 width b, and thickness t were subjected to quasi-static tensile loading using a universal testing machine. The longitudinal and transverse strains $d\varepsilon_{//}, d\varepsilon_{\perp}$ were recorded as:

$$\varepsilon_{//} = \Delta L/L_0,\ \varepsilon_{\perp} = \Delta b/b_0 \quad (5)$$

$$\nu = -d\varepsilon_{\perp}/d\varepsilon_{//} \approx -\varepsilon_{\perp}/\varepsilon_{//} \quad (6)$$

Fig. 6 - Tensile Test of Universal Testing Machine

The interaction between the macadamia husk and key machine components (e.g., 45# steel) depends primarily on elastic, frictional, and impact restitution properties, which were therefore experimentally determined and input into the DEM model. Based on the preceding mechanical tests (*Cai et al., 2025*), the static and dynamic friction coefficients, coefficient of restitution, density, and Poisson's ratio were obtained using the inclined-plane, free-fall, and density-measurement methods. After multiple repetitions and averaging, the final parameters used as EDEM inputs are summarized in Table 4.

Table 4

Contact Parameters

Material	Parameter	Value	Interaction	Parameter	Value
Green husk	Poisson's ratio	0.15	Husk–Husk	Restitution coefficient	0.24
	Density (kg m^{-3})	1050		Dynamic friction coefficient	0.3
	Shear modulus (Pa)	2.7e+07		Static friction coefficient	0.25
45# Steel	Poisson's ratio	0.3	Husk–Steel	Restitution coefficient	0.28
	Density (kg m^{-3})	7800		Dynamic friction coefficient	0.24
	Shear modulus (Pa)	2.1e+11		Static friction coefficient	0.32

Note. Physical and interaction parameters were obtained experimentally and used for DEM calibration. "–" indicates dimensionless values. ρ = density (kg m^{-3}); μs = static friction coefficient; μk = kinetic friction coefficient; e = restitution coefficient.

These values were obtained through experimental measurements using the inclined-plane sliding and rolling methods, and they reflect the specific surface conditions of the macadamia husks and steel *(Adama et al., 2022*). Compared to similar green husk materials, these physical parameters fall within the acceptable error range, confirming their reliability (*Chukwu et al., 2019*).These friction coefficients provide a more realistic representation of the interactions in the discrete element method (DEM) simulations and support the optimization of the dehusking process with greater accuracy.

Simulation Parameter Configuration

(1) Particle generation and gravity orientation

A dynamic particle generation approach was adopted in the DEM simulations. Particles were continuously injected within 1 second, and the total number corresponded to the experimental feed rate, The initial velocity of particles was set to –1 $m \cdot s^{-1}$ along the negative Z-axis in the model coordinate system. The gravity vector was assigned in the negative Y-axis direction.

(2) Contact models

Two models were mainly used:

① The Hertz–Mindlin (no slip) model

② The Hertz–Mindlin with JKR(Johnson–Kendall–Roberts) model

In this study, the Hertz–Mindlin with JKR model was applied to husk–husk contacts to account for adhesion, while the Hertz–Mindlin (no slip) model was adopted for husk–45# steel contacts.

(3) Nut geometry and solver configuration

To improve simulation efficiency and control computational cost, the geometry of the macadamia husk was simplified from an irregular shape to an equivalent sphere. To confirm that this geometric simplification does not introduce excessive errors, a repose angle verification test was subsequently conducted, demonstrating that the relative deviation remained within acceptable engineering limits

The tuning objective was to maintain the maximum contact overlap within the acceptable engineering range while ensuring efficient computation. In this study, the maximum overlap was set to 3 %.

(4) Angle of Repose Verification Test

After completing the calibration of parameters for macadamia nuts and 45# steel, verification was conducted using a cylinder lifting test, which is a standard method for validating DEM contact parameters.

Fig. 7 - Cylinder lifting test for angle of repose measurement

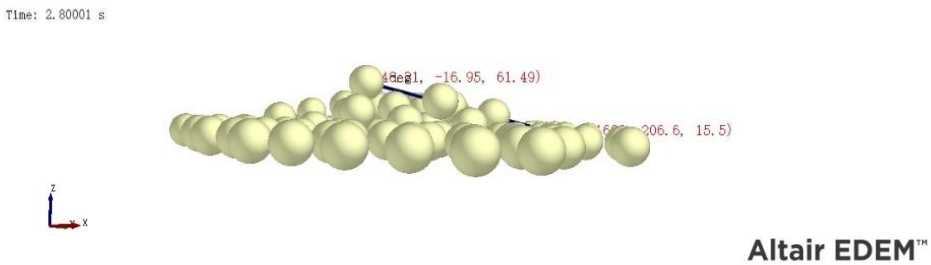

Fig. 8 - DEM simulation of the angle of repose test

The physical repose angle was 10.4°, while the simulated repose angle was 11.7°, resulting in an absolute error of 1.3°. This small deviation confirms that the calibrated DEM parameters were physically reasonable and suitable for subsequent simulations.

Simulation Results and Analysis

Three time intervals were selected to analyze the velocity distribution and stress conditions of macadamia particles within the peeling drum *(Toba et al., 2020)*.

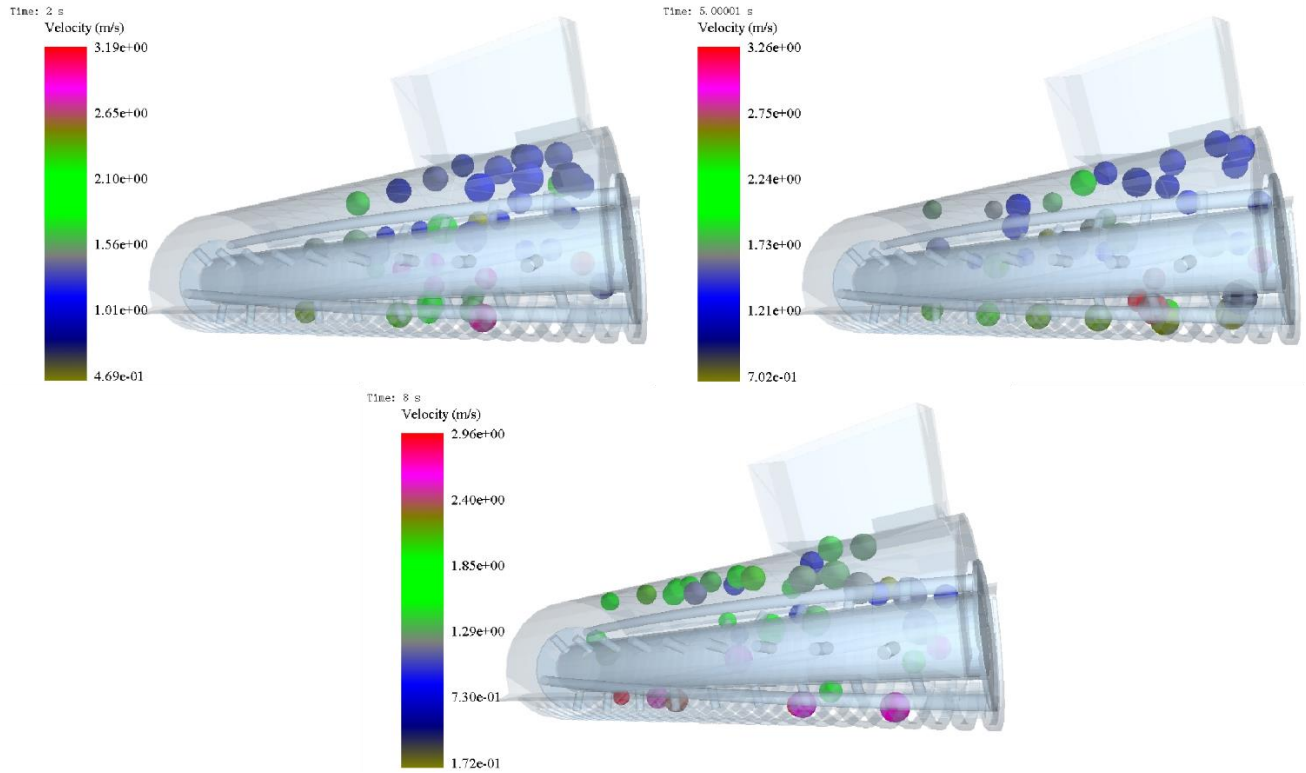

Fig. 9 - Macadamia Green husk Simulated Motion Trajectory

At the initial stage, particle velocities ranged from 0.47 to 3.19 m·s⁻¹, indicating that the particles were in the acceleration phase as they transitioned from rest to motion. At 5 s, the velocity distribution changed significantly. Particles migrated toward the outlet, and their velocities increased substantially, reaching up to 3.26 m·s⁻¹, while exhibiting distinct stratification and aggregation phenomena. By 8 s, the particle distribution became more uniform, with velocities converging to a narrower range of 0.17–2.96 m·s⁻¹. At this stage, particle motion reached a quasi-steady flow regime, resulting in a stable overall velocity field.

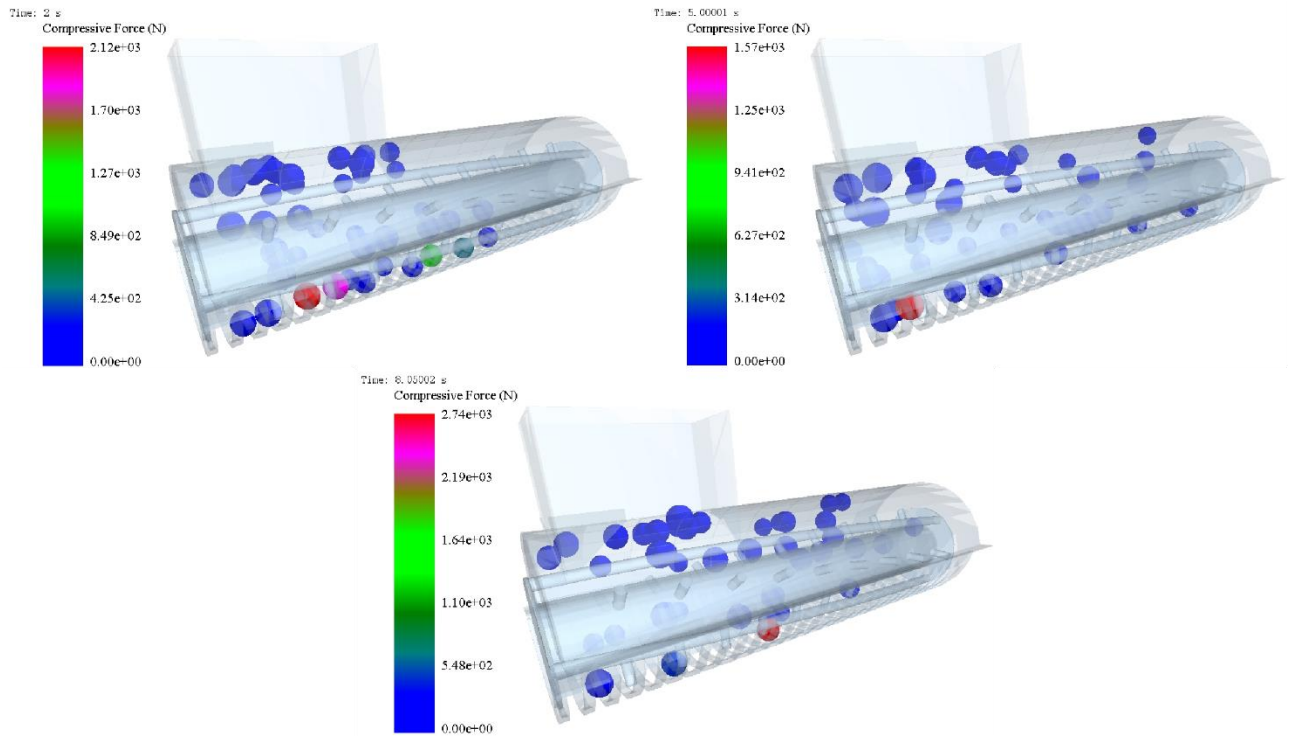

Fig.10 - Schematic Diagram of Force on Macadamia Green husk

At 5 seconds, the compressive forces were more uniformly distributed overall. By 8 seconds, the compressive force range expanded to 0–2.74 × 10³ N, with several distinct stress concentration zones forming near the outlet, helping to minimize the risk of nut damage.

In summary, the EDEM simulation effectively reproduced the macadamia green husk peeling process. Combined analysis of the velocity and stress fields revealed a characteristic evolution pattern of "initial local concentration – mid-phase uniformity – terminal aggregation." Validating the accuracy and applicability of the DEM model.

Based on the simulation outcomes and prior experimental data, the effective peeling force for macadamia green husk can be defined within the range of 300–2000 N *(Xue et al., 2014)*

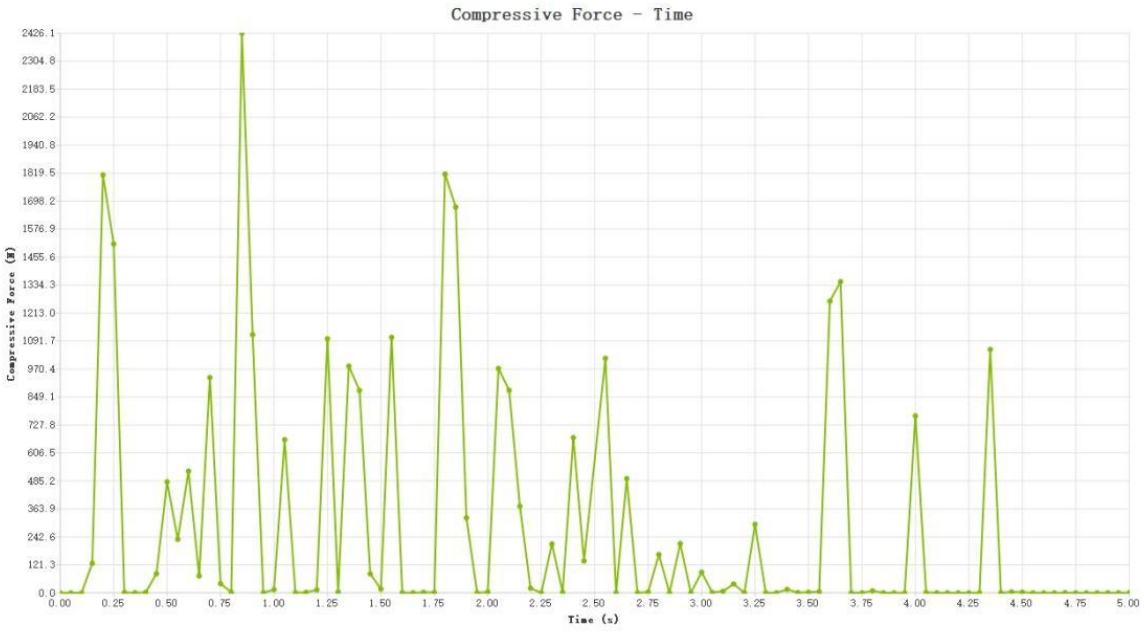

Fig. 11 - Stress Variation Diagram of Macadamia Green husk Simulation

Fig.11 shows the time history of compressive forces for a randomly selected particle. During one observation period, out of 39 recorded force events, only one exceeded 2000 N. The nut breakage rate of the equipment was controlled below 2.56 %.

These results provide strong data support for optimizing the design and performance of the peeling machine.

RESULTS

Materials and Experimental Design

Macadamia nuts (cultivar series "A4") were harvested from Lincang, Yunnan Province, China. A total of 27 experimental runs were conducted to evaluate the mechanical properties of green-husked macadamia nuts. Defective samples (mold, mechanical damage, abnormal morphology) were excluded from the experiments.

A total of 17 experimental runs were conducted to optimize the dehusking parameters—drum speed, feed rate, and minimum spacing—and to evaluate their effects on dehusking performance.

All experiments were carried out in August 2025 at Southwest Forestry University.

Box–Behnken Design

The Box–Behnken design (BBD) was used to optimize the key process parameters. Based on the results of both mechanical testing (27 runs) and peeling simulations (17 runs), the BBD enabled efficient evaluation of the interactions among variables and their effects on dehusking performance *(Yu et al., 2024)*.

Experimental Implementation and Factor Coding

Bench tests followed a BBD matrix with three factors: A-drum speed (r min^{-1}), B-feed rate (kg min^{-1}), and C-minimum spacing (mm). Center points were replicated four times to estimate pure error and assess stability.

All runs were randomized. Before each run, speed, feeding mechanism, and gap were re-calibrated. Dehusking rate was defined as the proportion of nuts dehusked without nut damage in a single run.

Table 5

Experimental Factor Coding

Level	Factor		
	A: Speed（r min⁻¹）	B: Feed rate（kg min⁻¹）	C: Minimum spacing *(Ali et al.)*
–1	200	3.9	6
0	300	6.3	8
1	400	9.9	10

Note. The coded levels −1, 0, and +1 correspond to the low, center, and high values of each factor in the Box–Behnken design.

ANOVA Results and Model Significance

Table 6

Experimental Design Scheme and Results

Run	Factor			Dehusking rate（%）
	X_1	X_2	X_3	
1	–1	–1	0	71.4
2	1	–1	0	99.9
3	–1	1	0	60.0
4	1	1	0	99.9
5	–1	0	–1	37.5
6	1	0	–1	87.5
7	–1	0	1	37.5
8	1	0	1	99.9
9	0	–1	–1	99.9
10	0	1	–1	85.0
11	0	–1	1	99.9
12	0	1	1	60.0
13	0	0	0	99.9
14	0	0	0	99.9
15	0	0	0	87.5
16	0	0	0	99.9
17	0	0	0	85.0

Note. Center points were repeated four times for error estimation.

In Table 6, the center-point dehusking rate fluctuates by 24.9 percentage points (85.0%–99.9%). It falls within the anticipated error range. To enhance the robustness of the statistical analysis, the data were weighted.

The preliminary regression model was simplified by removing non-significant interactions and quadratic terms. The final model is as follows:

$$Y = 0.821+0.223A-0.014B+0.014C+0.718A^2$$

Table 7

Analysis of Variance for Skin Breakage Rate

Source	Sum of Squares	df	Mean Square	F–value	p–value	
Model	0.6593	9	0.0733	6.16	0.0128	*
A–A	0.3965	1	0.3965	33.32	0.0007	*
B–B	0.0518	1	0.0518	4.36	0.0753	ns
C–C	0.0023	1	0.0023	0.1914	0.6749	ns
AB	0.0032	1	0.0032	0.273	0.6174	ns
AC	0.0033	1	0.0033	0.2778	0.6144	ns
BC	0.0156	1	0.0156	1.31	0.2895	ns
A	0.1073	1	0.1073	9.01	0.0199	*
B	0.0082	1	0.0082	0.6889	0.4339	ns
C	0.0664	1	0.0664	5.58	0.0501	~
Residual	0.0833	7	0.0119			
Lack of Fit	0.0635	3	0.0212	4.27	0.0973	~
Pure Error	0.0198	4	0.005			
Cor Total	0.7426	16				

Note: p < .05(significant); p < .01(highly significant); p < .001(extremely significant); † or ~ p < .10(marginally significant); ns —— not significant (not significant)

ANOVA was performed based on the quadratic regression model for dehusking efficiency using Design-Expert 13.0.

As shown in Table 7, the overall model is significant (F = 4.55, p = .0291 < 0.05), indicating that drum speed, feed rate, and minimum gap exert statistically significant effects on the dehusking rate within the tested range. And the adjusted $R^2 \approx 0.731$ indicate that about 73.1 % of the response variance is explained by the model, demonstrating good fitting performance.

Regarding single-factor significance, drum speed (A) exhibits a highly significant effect on the dehusking rate (p = .0018 < 0.01) and is thus the dominant factor. Dehusking rate increases notably with higher speed. Feed rate (B) and minimum gap (C) show p-values of 0.2064 and 0.6878 respectively, both insignificant. The interactions AB, AC, and BC are not significant. The quadratic term A^2 is marginally significant (p = .0598).

The lack-of-fit p-value (0.0522 > 0.05) indicates a good model fit. This shows that the regression model accurately describes the observed experimental trends.

Overall, the dehusking rate is mainly governed by the primary effect of drum speed. The strong linear effect of speed dictates the global response trend.

Response-Surface Analysis

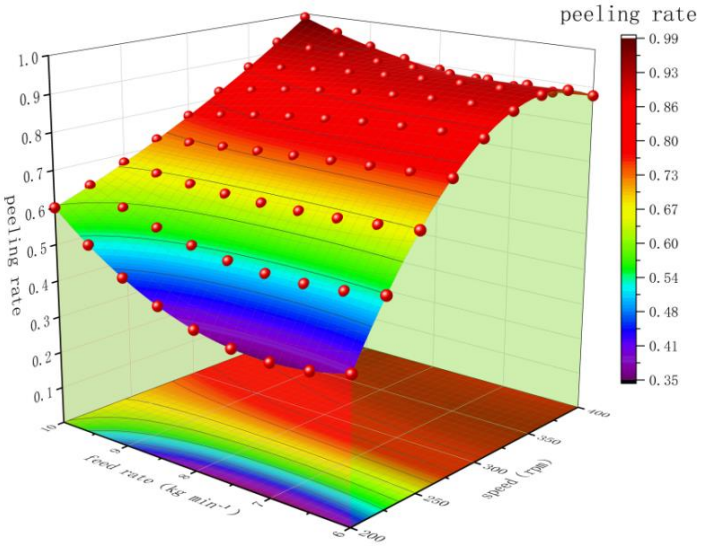

Fig. 12 - Speed–Feed Rate Response Surface

As shown in Fig.12, the surface rises nearly monotonically, and the steepest-ascent direction is essentially along the speed axis; indicating a pronounced main effect of speed on the response *(Tuoheti et al., 2021)*. With increasing speed, a continuous high-value plateau (≈0.88–0.89) appears in the upper-right region, suggesting entry into a performance saturation zone; changes in feed rate produce only minimal marginal effects. Gains across the speed direction reach ≈0.04–0.09,The measured points fit the modeled surface well *(Chen et al., 2023)*.

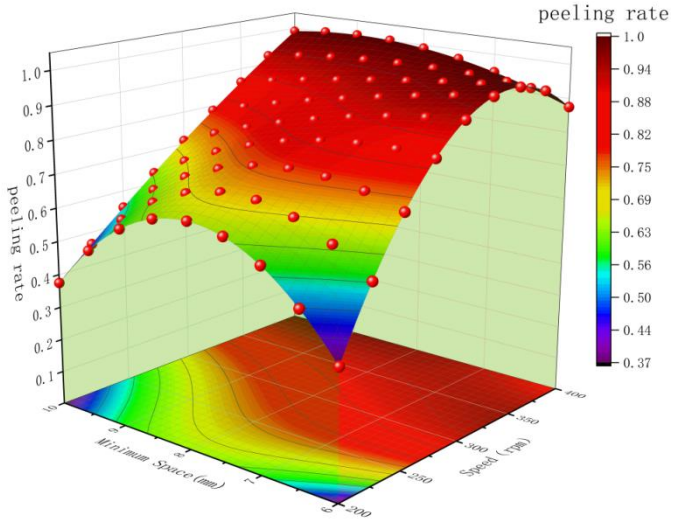

Fig. 13 - Speed–Minimum Spacing Response Surface

As shown in Fig.13, the overall trend is dominated by speed. A broad, flat high-value region (≈0.88–0.89) emerges at the high-speed side. Speed has a significant leading effect on the dehusking rate. Within the studied range, every +100 r min⁻¹ increases the mean dehusking rate by about 0.045–0.050. When speed exceeds 380 r min⁻¹, the surface becomes progressively flatter, indicating that the dehusking rate is approaching a saturation region and is no longer sensitive to further increases *(Zhang et al., 2023)*.

The minimum-gap direction exhibits a shallow trough or saddle curvature near the mid-level, with slight rises on both sides. However, the amplitude of this local extremum is small its contribution to the overall variation is clearly weaker than that of the dominant speed effect *(Rodrigues, 2021)*.

Drum speed is the dominant factor. Forms a continuous, flat high-value plateau at the high-speed side. Within the investigated range, the main variation in response is driven by speed, the overall pattern shows a stable “high-speed tolerant zone” morphology *(Lian et al., 2023)*.

Parameter Optimization and Model Validation

The regression model was simplified by removing the non-significant interaction and quadratic terms. The final model is expressed as follows:

$$Y = 0.821+0.223A-0.014B+0.014C+0.718A^2$$

The coefficient of determination is $R^2 = 0.834$ and the adjusted coefficient $R^2_{adj} = 0.791$.

While the effects of minimum gap and feed rate are weaker.

The results show that when A = 0.67, B = 0.1, and C = 0.5, the dehusking rate reached 0.95–0.99, while the nut damage rate remained low and stable. The recommended engineering operating window is a drum speed of n = 300-400r min⁻¹, a minimum gap of 9-10mm, and a feed rate of 6–10 kg min⁻¹. Under these conditions, both dehusking efficiency and nut integrity achieve an optimal combined performance (*Shi et al., 2019*).

A validation test was subsequently conducted under the following conditions: drum speed of 400 r min⁻¹, minimum gap of 9.5 mm, and feed rate of 6.3 kg min⁻¹. A total of 198 macadamia nuts (cultivar “A4”) were used in the test. The experiment was performed in three independent runs, with 66 nuts per run and a continuous feeding duration of 10 s.

Table 8

Comparison of Real Machine Verification Results

Metric	Predicted Value	Measured Mean	Relative Error / %	Remarks
Dehusking Rate / %	95.0	95.4	0.4	Model prediction is accurate
Nut Damage Rate / %	4.1	4.76	0.66	Slightly higher than the predicted value
Machine Stability	—	good	—	Smooth operation without clogging

Note. The optimized parameters were validated through physical experiments under identical working conditions.

As shown in Table 8, the measured dehusking rate was 95.4 %. The nut damage rate was 4.76 %. The equipment operated smoothly, without noticeable clogging or overload.

CONCLUSIONS

This study established a mechanical framework for “horizontal single-drum guided-extrusion” dehusking and clarified the cooperative crack-initiation mechanism between normal compression and tangential friction within the slit formed by the drum and the supporting plate.

Three-factor, three-level experiments showed that the equivalent dehusking force of macadamia green husk ranges from 0.30 to 2.00 kN, with significant anisotropy under different loading orientations: approximately 2.3 kN in the normal direction, 1.9 kN along the hilum line, and 0.9 kN in the lateral direction. These results provide a theoretical basis for drive selection and safety margin determination.

The discrete element method (DEM) simulation agreed well with the experimental measurements, with an error of approximately 1.3°. The velocity field evolved from an initial acceleration stage to a quasi-steady-state flow regime. The maximum compressive force reached approximately 2.74 kN, while contact events exceeding 2.0 kN accounted for about 2.56% of the total. Under these conditions, high dehusking efficiency and low nut damage can be achieved simultaneously.

Significant dehusking-rate model, with drum speed as the dominant factor ($p = 0.0018$), feed rate and minimum gap exhibited weaker main effects. The response surface “high-speed tolerant zone” , a stable high-value plateau near $n \approx 400$ r min^{-1}, insensitive to fluctuations in feed rate and gap.

An engineering operation window is therefore proposed: a drum speed of 300–400 r min^{-1}, with a minimum gap of 9–10 mm, which can stably achieve a dehusking rate ≥0.90.

The reliability of the model was verified experimentally. Under the optimal parameter combination (400 r·min^{-1} drum speed, 9.5 mm minimum gap, and 6.3 kg·min^{-1} feed rate), the measured dehusking rate reached 95.4%, while the nut damage rate was 4.76%. The integrated optimization approach effectively controls nut damage while maintaining high dehusking efficiency.

Overall, the system demonstrates high operational stability and practical applicability, providing a useful theoretical reference for the design and optimization of macadamia green-husk removal equipment.

ACKNOWLEDGMENTS

This research was supported by the Scientific Research Fund of the Yunnan Provincial Department of Education, China (Grant No. 2025Y0851).

The authors also acknowledge the support from the College of Mechanical and Transportation Engineering, Southwest Forestry University, for providing experimental facilities and testing equipment.

Special thanks are extended to Professor Daigen Zhu for his valuable guidance throughout the study and to the technical staff for their assistance in conducting the experiments.

REFERENCES

[1] Adama, J. C., Arocha, C. G., & Ogbobe, P. O. (2022). Determination of some physical properties, angles of repose and frictional properties of a local variety of kernel and nut of oil palm. *Nigerian Journal of Technology, 41*(2), 365-369. doi:10.4314/njt.v41i2.18

[2] Ali, Shajia Afrin, Sonego, Marilia, Salavati, Mohammad, & Fleck, Claudia. (2023). Influence of Structure and Geometry on the Compressive Deformation Behavior of Macadamia Integrifolia and Bertholletia Excelsa Shells: A Validated Finite Element Simulation Study. *Advanced Engineering Materials, 26*(4). doi:10.1002/adem.202300723

[3] Cai, Z., Wang, Y., Li, L., Xu, L., Li, X., Wang, W., et al. (2025). Design and test of a spiral inclined green walnut peeling machine based on EDEM. *Storage and Process*. *25*(05), 92-101.

[4] Chen, X., Li, W., Bai, X., & Xu, D. (2023). Experimental study on the mechanical characteristics of green-husk cracking in Xiangling walnut. *China Oils and Fats*. 48(11), 135-140. doi:10.19902/j.cnki.zgyz.1003-7969.220446

[5] Chukwu, P., Uzoigwe, F. C., Chukwuezie, O. C., & Nwakuba, N. R. (2019). Friction Coefficients of Local Food Grains on Different Structural Surfaces. *Journal of Engineering Research and Reports*, 1-9. doi:10.9734/jerr/2019/v6i316951

[6] Hadi, Ahmed, Roeplal, Raïsa, Pang, Yusong, & Schott, Dingena L. (2024). DEM Modelling of Segregation in Granular Materials: A Review. *KONA Powder and Particle Journal, 41*(0), 78-107. doi:10.14356/kona.2024017

[7] Han, Z., Yang, Y., Jiang, J., Wang, Y., Ou, Y., & Li, J. (2024). Development of a macadamia green-husk shelling machine. *Farm Machinery Using and Maintenance*. (08), 19-21+26. doi:10.14031/j.cnki.njwx.2024.08.005

[8] Hlavangwani, Neftal, Tartibu, Lagouge, & Adebo, Oluwafemi. (2025). Development, Construction, and Testing of a Dehulling Machine. *International Journal of Engineering Trends and Technology, 73*, 397-409. doi:10.14445/22315381/IJETT-V73I1P134

[9] Jiang, K., Chen, Z., Li, Y., Zhang, H., & Zhao, M. (2021). Simulation of mechanical characteristics of peeling rollers for macadamia peeling machines. *Food and Machinery*. *37*(08), 110-114. doi:10.13652/j.issn.1003-5788.2021.08.018

[10] Li, H., Wu, W., Tang, J., & Wu, H. (2025). Research on the analysis of peeling movement of spiral kneading peeling machine based on discrete elements. Science and Technology of Cereals, *Oils and Foods*. *33*(03), 172-181. doi:10.16210/j.cnki.1007-7561.2025.03.017

[11] Lian, W., Xi, H., Zhang, F., Liu, X., & Bao, E. (2023). Drop-impact analysis and parameter optimization of key components in green walnut dehulling devices. *Journal of Chinese Agricultural Mechanization*. *44*(06), 89-96. doi:10.13733/j.jcam.issn.2095-5553.2023.06.013

[12] Ma, S., Hu, X., Fu, J., Zhang, X., Zhou, Y., Huang K., Wei Y., Yang Y., Jiang J., Wang J., He X., Guo G. (2025). Quality analysis and comprehensive evaluation of macadamia fruits in Yunnan. *Science and Technology of Food Industry*. *46*(07), 259-271. doi:10.13386/j.issn1002-0306.2024050032

[13] Rodrigues, Antonio Carlos. (2021). Response Surface Analysis: A Tutorial for Examining Linear and Curvilinear Effects. *Revista de Administração Contemporânea, 25*(6). doi:10.1590/1982-7849rac2021200293.en

[14] Shi, G., Ning, D., Zhong, T., & Pan, B. (2020). Process technology study on key design stages of a macadamia green-husk peeling machine. *Agricultural Development and Equipment*. (09), 33-34.

[15] Shi, Z., Xu, Y., Zhou, J., Wang, Y., & Zhao, H. (2019). Numerical simulation and mechanical analysis of peeling rollers in walnut green-husk peeling machines. *Machine Tool & Hydraulics*. *47*(19), 136-139+152.

[16] Toba, Ange-Lionel, Griffel, L. Michael, & Hartley, Damon S. (2020). Devs based modeling and simulation of agricultural machinery movement. *Computers and Electronics in Agriculture, 177*, 105669. doi:https://doi.org/10.1016/j.compag.2020.105669

[17] Tuoheti, R., Ge, Q., Liang, Z., Zhou, L., & Ma, Q. (2021). Implementation of multi-factor design ANOVA and analysis of multi-factor coupling effects. *China Occupational Medicine*. *48*(04), 447-450+456.

[18] Walton, David A., & Wallace, Helen M. (2015). The effect of mechanical dehuskers on the quality of macadamia kernels when dehusking macadamia fruit at differing harvest moisture contents. *Scientia Horticulturae, 182*, 119-123. doi:10.1016/j.scienta.2014.10.053

[19] Wang, S., Pan, R., Xue, Z., He, F., Fan, J., & Han, S. (2022). Design and experiment of an extrusion-type macadamia dehusking device. *Journal of Agricultural Mechanization Research*. *44*(10), 60-66. doi:10.13427/j.cnki.njyi.2022.10.011

[20] Xue, Z., Huang, Z., Guo, X., & Zhang, Q. (2014). Experimental study on shear mechanical properties of macadamia nuts. *Transactions of the Chinese Society for Agricultural Machinery. 35*(02), 85-88+135. doi:10.13733/j.jcam.issn.2095-5553.2014.02.021

[21] Yang, Y., Duan, M., Zhang, B., Yan, S., Shi, W., Yang, F., Pan, L., Zhou X. (2024). Research progress on macadamia processing and comprehensive utilization of industrial by-products. *China Oils and Fats*. *49*(12), 100-104. doi:10.19902/j.cnki.zgyz.1003-7969.230123

[22] Yu, Y., Li, P., Lai, Q., Tan, Y., Zhao, Q., & Chen, Y. (2024). Simulation and experiment of coffee harvesting process based on DEM–MBD coupling. *Transactions of the Chinese Society for Agricultural Machinery*. *55*(S2), 157-167.

[23] Zhang, G., Chen, L., Guo, Z., Liu, H., Dong, Z., & Liang, F. (2023). Design and experiment of a combined peeling machine for water chestnut. *Sci Rep, 13*(1), 2393. doi:10.1038/s41598-023-28472-9

[24] Zhao, D., & Wang, Y. (2025). Analysis of mechanical properties of green-husk cracking force in Yangbi walnut. *Agricultural Equipment & Technology*. *51*(02), 52-55.